

Radioiodination, Molecular Modelling and Biological Evaluation of Aniracetam as a Tracer for Brain Imaging

M. H. Sanad¹, A. B. Farag², Dina H. Salama³

¹Labeled Compounds Department, Hot Labs Center, Atomic Energy Authority, P.O. Box 13759, Cairo, ²Pharmaceutical Chemistry Department, Faculty of Pharmacy, Ahrum Canadian University, Giza, ³ Health Radiation Research Department (Radiodiagnosis Unit), National Center for Radiation Research and Technology, Atomic Energy Authority, Cairo, Egypt

THE PRESENT study focused on synthesis of radioiodinated aniracetam for a potential brain imaging. Aniracetam (AN) has been labeled using [¹²⁵I] with chloramine-T (Ch-T) as an oxidizing agent. The key effective factors such as amount of oxidizing agent, amount of substrate, pH, reaction temperature and reaction time, have been systematically studied to get high radiochemical yield of the radioiodinated aniracetam. The obtained results show a high radiochemical yield of iodoaniracetam that reached 98%. The labeled compound was separated and purified using thin layer chromatography (TLC), paper electrophoreses and high performance liquid chromatography (HPLC). Docking and modeling with AMPA receptors, gamma camera and drug inhibition were studied. In vivo biodistribution of radioiodinated aniracetam was evaluated in Swiss albino mice. The biodistribution results show a brain uptake that reached 9.50 ± 0.17 %ID/g at 15 min post injection (p.i.). Based on these results, it can be stated that radioiodinated aniracetam could be efficiently used as a potential radiotracer drug for brain imaging.

Keywords: Radioiodinated Aniracetam, Brain Imaging, Gamma Camera, Molecular Modeling and Docking

Introduction

There are many techniques that are used in brain imaging or neuro imaging (Thomas et al., 1984; Heilbrun et al., 1987; Levivier et al., 2004; Eggebrecht et al., 2012) et al., 2012; Silberstein, 2000; Farid et al., 2012; Bateman et al., 2012). Iodine -123 is the isotope of choice for medical imaging ¹⁰ with a half-life of 13.22 h. and decays by emission of gamma radiation with energy of 159 keV. However, its short half-life and high expenses lead to using iodine-125 to develop the labeling procedure and evaluate the biodistribution in mice (Bruno and Nicolaus, 1982; Hupf et al., 1968; Venkat et al., 1992). Therefore, iodine-131, (Simon et al., 2006) a radioactive isotope is considered more suitable than iodine-123 in imaging process, due to its low expenses compared to others. Brain imaging diseases require the selection of certain compounds with high binding affinity to selective receptors such as AMPA receptor in case of aniracetam (Maina

et al., 1989 and Stensbol et al., 2002). There are three types of receptors (α -amino-3-hydroxy-5-methyl-4-isoxazolepropionic acid receptor) which is considered glutamate subsections that are known as thrilling ones, while kainate and NMDA (N-methyl-D-Aspartate) are the rest ones (Eleore et al., 2005 and Bowie, 2012). Glutamate subsections (AMPA) intermediate enhance the excitation and transmission of amino acid. In addition, they are considered heterogeneously represented in the brain with eight possible subunits (Ozawa et al., 1998). The aim of the work is to prepare a radioiodinated aniracetam (Fig. 1&2) as a potential radiotracer drug to overcome the defects resulted from other radiotracers such as low brain uptake and small brain to blood ratio. A group of Swiss Albino mice was injected with radioiodinated aniracetam intravenously at different times. In this study, ¹³¹I-aniracetam was detected in brain using gamma camera detection and compared with ^{99m}Tc-tricarboxyl oxiracetam

complex, $^{99m}\text{Tc}(\text{CO})_3\text{-5HTIDA}$, $^{99m}\text{Tc}(\text{CO})_3\text{-DEDT}$, $^{99m}\text{Tc}(\text{CO})_3\text{-OH-PP-CS}_2$, $^{99m}\text{Tc-ECD}$, and $^{99m}\text{Tc-HMPAO}$.

Experimental

Materials and Methods

Reagents

Sodium iodide radiotracer Na^{125}I (185 MBq/50 μL) was purchased from the institute of isotopes, Budapest, Hungary. It was diluted into 0.04M NaOH, pH 9-11. In addition sodium [^{131}I] iodide (3.8 GBq/mL) diluted in 0.05 M NaOH, pH 8 to 11 for radiolabeling was given as a gift from RPF, Atomic Energy Authority, Egypt. Aniracetam, Chloramine-T [N-chloro-p-toluene sulfonamide salt (Ch-T)], ethanol, Tetrahydrofuran and methanol were purchased from Sigma-Aldrich. Thin layer chromatography (TLC) aluminum sheets (20 \times 25 cm) SG-60F254 were supplied by Merck. Whatman paper number (PC) 1, was supplied from Whatman International Ltd, Maidstone, Kent, UK. All chemicals were of analytical or clinical grade and were used directly without further purification unless otherwise stated. Double distilled water was used for the preparation of solutions, dilution and washing purposes.

Apparatus

All reactions were followed by TLC (Silica gel, Aluminum Sheets 60 GF₂₅₄, Merck), and were detected with a NM UV lamp. A well-type NaI scintillation γ -Counter model Scalar Ratemeter SR7 (Nuclear Enterprises Ltd., USA) was used for radioactive measurement; pH meter: model 601. A digital ion analyzer (Orion Research, USA); ionization chamber: model CRC-15R (Capintec, USA); precision electronic balance: model HA 120 (MAD Company Ltd., Japan); stirring hot plate: model 210 T Thermix (Fisher, USA); electrophoresis apparatus: E.C. Corporation (Albany, OR, USA). The mixture was completely purified using high performance liquid chromatography (HPLC) with the column (RP-C₁₈-250 mm \times 4.6 mm, 5 μm , LiChrosorb) using a Shimadzu model detector SpD-6A model which consists of pumps LC-9A, Rheodyne injector and UV spectrophotometer detector at 285 nm wavelength. Methanol: water (60:40) was used as mobile phase with a 1.0 mL min^{-1} flow rate (Kamlesh *et al.*, 2016). The Dose mice Calibrator was used for measuring the radioactive dose administered to the mice by a Well Ion Chamber Detector, manufactured by Capintec Company, USA. The gamma camera with a 5-mm pinhole

collimator, window setting of 190 keV, and 20 % width, Dual-Head Variable Angle Gamma from Siemens, in the Nuclear Medicine Unit of the National Cancer. Institute, Cairo University, Egypt, was used in the present work.

Radiolabeling of Aniracetam

Radiolabeling process was carried out in a two-neck, 25 ml round bottomed flask fitted with a reflux condenser on one neck and the other neck was fitted with rubber stopper for withdrawing samples. The flask was immersed in a thermostatically controlled water bath. No-carrier-added Na^{125}I was transferred to the reaction system and evaporated to dryness by vacuum. Accurately weighed 50 μg Ch-T dissolved in ethanol (1:1) was added to the reaction flask, and then aniracetam 100 μg was dissolved in ethanol (1:1) at ambient temperature for 30 min. The reaction mixture was stirred with a magnetic stirrer at pH 6 and left in room temperature for 30 min. Then 100 μL of (60 mg/ml) sodium metabisulphite (MBS) was added to decompose the excess of iodine in order to stop the reaction and the radioiodinated product was isolated. The reaction mixture volume was fixed to ~ 700 μL . The radiochemical yield percentage was determined using TLC and paper electrophoresis and completely purified using HPLC column.

Gamma Camera Imaging

The body distribution profile in mice was recorded in the gamma camera with a 5-mm pinhole collimator, window setting of 190 KeV, and 20% width for gamma-imaging studies. After intravenous administration of [^{131}I] radioiodinated aniracetam (injected dose: 0.1mg aniracetam in 0.5mL phosphate buffer (pH 6), activity: 0.2 mCi), the animal was anesthetized by intramuscular injection of xylazine (10.0 mg/kg) and 0.5 mL of ketamine hydrochloride (100.0 mg/kg) for 5min before imaging. The doses were given according to Laboratory Animal Sciences Program in NCI Fredric Center for Cancer Research, and this anesthetic agent is believed to have a negligible effect on both blood pressure and the biodistribution of the radiolabeled samples. The animals were fixed promptly on a board in the posterior anterior position and imaging was performed at different time intervals using a gamma camera. The images were taken in the two positions anterior and posterior. Gamma camera images were acquired at 5, 15, 30, 60, 120, and 240min after injection. The static

images were stored in a 512x512 matrix size and acquisition times were 300s. Scintigraphy was the diagnostic nuclear medicine test used in this study, where [^{131}I]iodoaniracetam was administered intravenously and the emitted gamma radiation captured by the gamma camera (Philips axis gamma 2) to form two-dimensional images.

Different Analytical Techniques

A thin layer chromatography was used to separate the free iodide from the labeled compound to get high radiochemical yield. Using TLC-SG60 F₂₅₄, the sheets were marked at 2 cm from the base with 1 cm lining fragments up to 16 cm using non-pointed pencil 2-5 μL . The reaction mixture was spotted using micropipette at the origin then the thin layer chromatography sheets were developed using a fresh mixture of chloroform: ethanol (9:1v/v) as described by author name. Another separation process was performed by paper electrophoresis analysis according to Sanad et al., (2016). The analysis shows that labeled

compound remained at zero point indicating its neutrally charged nature while, free radioiodide (I^-) moved towards the positive electrode (+) with 12 cm distance (Fig.3). Finally, HPLC was used, in which 10 μL aliquot of the radioiodinated aniracetam mixture was injected into the column using the flow rate and the mobile phase mentioned above. Hence, fractions of one mL were collected separately using a fraction collector up to 15 mL and counted in a well-type- γ -scintillation Counter. The data obtained from HPLC analysis show that the retention time R_t of free iodide and radioiodinated aniracetam were found at 3.5 and 8 min, respectively, and UV of aniracetam was given at 5.91 min. (Fig.4). Differences in the retention times (R_t) between UV of aniracetam and radioiodinated aniracetam may be due to increasing of the hydrophobicity of labeled compound upon incorporation of iodine in aromatic rings which leads to these differences in R_t (Sanad et al., 2017 and Kamlesh et al., 2016).

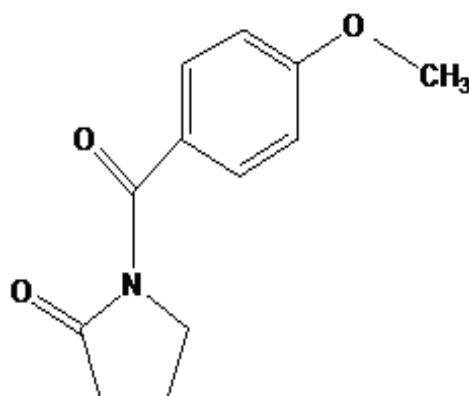


Fig.1. The chemical structure of aniracetam

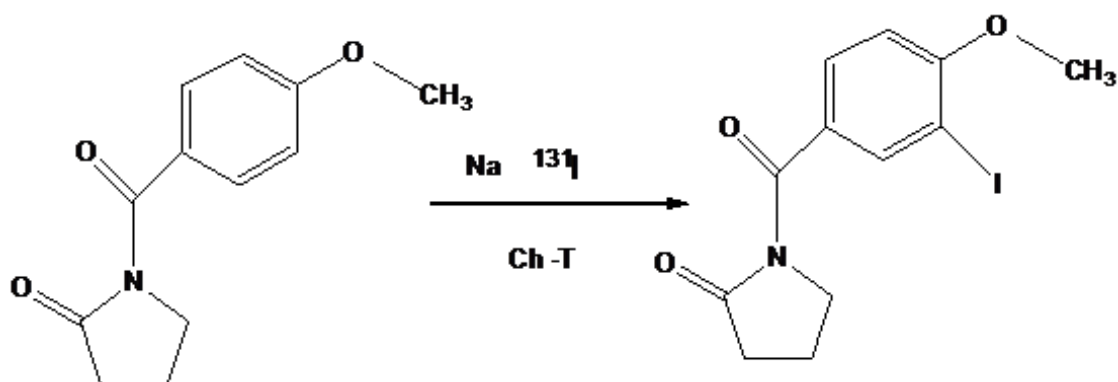


Fig.2. The proposed structure of radioiodinated aniracetam

Animal and biodistribution studies of the [¹²⁵I] aniracetam.

This procedure occurred and set out according to animal ethics committee approved at Labeled Compounds Department, Egyptian Atomic Energy Authority. Normal Swiss Albino mice (30-40 g) were intravenously injected in tail, with 0.1 μ L (7.2 MBq) of purified radiotracer ¹²⁵I-AN. They kept alive in metabolic cages, under normal conditions, for different periods of time. In addition, the quantitative determination of organ distribution, tissue samples for 5 animals at each post-injection time points were weighed and counted. Quantitative determination of organ distribution can be approved using, five mice for each experiment and the mice were sacrificed at different time intervals post-injection (p.i.) at (5, 15, 30 min, 1, 2 and 4 hr). Then, different organs were first removed then counted. The count of the total injected volume of radiolabeled compound was compared to the count of a standard solution of ¹²⁵I-AN. It was approved that the following organs such as bone, blood, and muscles were supposed to be 10, 7, and 40 %, respectively, of the total body weight. The samples were compiled in pre-weighed vials and counted. The rest organs then, were removed counted and compared to a standard solution of the complex. Finally, the uptake of each organ can be calculated as a percentage of the injected dose per gram (% ID/gram \pm SD). The data were estimated with one way ANOVA test. Results for *P* were reported and all the outcomes were given as mean \pm SD. The level of importance was set at *P* < 0.05 (Sanad et al., 2016).

Determination of the Partition Coefficient for the [¹²⁵I]Aniracetam

The octanol/water partition coefficient of [¹²⁵I] aniracetam was determined at pH value of 7.4 by measuring its distribution in n-octanol and phosphate buffered saline (PBS), respectively. A sample of 100 μ L was added to an immiscible liquid containing PBS (900 μ L; pH 7.4) and n-octanol (1 mL), then after 5 minutes vigorous vortex, the mixture was incubated for 30 minutes at room temperature. Centrifugation at 5000rpm for 5 minutes ensured complete separation of the organic and the aqueous layers. An aliquot (100 μ L) from each layer was measured using a γ counter. The partition coefficient value can be expressed as log $P_{o/w}$ values and repeated for five times.

Stability in Two Different Media

The stability in two different media such as human serum and saline has been evaluated as follows: In serum, a purified radioiodinated

aniracetam was determined by mixing 0.2 ml of radiotracer solution with 0.8 ml serum and kept at ambient temperature. In addition, radioiodinated aniracetam [5 μ L (3.20 MBq)] was checked in saline. At time intervals, the stability of radioiodinated aniracetam in two different media was assayed using TLC or HPLC technique, and counted in a well-type γ -scintillation counter (Sanad et al., 2016).

Drug Inhibition Study of Labeled Compound

Different amounts of unlabeled aniracetam were used in the range of (0–1000 μ g), after that the animals were injected, 15 min prior to the injection of radioiodinated aniracetam, then the percentage of brain uptake was evaluated at 15 min post-injection of radioiodinated aniracetam (n=5) (Sanad et al., 2016 and Amin et al., 2013).

Molecular Modeling

The docking emulation can be achieved using the x-ray crystallographic composition of AMPA (PDB code: 4UQK) bound to the inhibitor QUS (s)-2-Amino-3-(3,5-dioxo-[1,2,4]oxadiazolidin). The PDB file was restored from Protein Data Bank. Chains B, C and D were deleted and structure of chain A was processed using the Structure Preparation application in Molecular Operating Environment (MOE), 2008.10. Subsequently, the protonate 3D application of MOE was used to add the missing hydrogens and properly assign the ionization states (Molecular Operating Environment (MOE), 2008; Labute, 2008; Naïm et al., 2007). The resultant model was further refined by energy minimization to a gradient of 0.01 kcal mol⁻¹ Å⁻¹ keeping atoms tethered within 0.5 Å from their crystal structure positions. The default procedure in the MOEDock application was used to find the favorable binding configurations of the studied ligands. Initial placement poses generated by the Alpha Triangle matcher were rescored and filtered using the London dG Scoring method to pick those exhibiting maximal hydrophobic, ionic, and hydrogen-bond contacts to the protein. This was followed by a refinement stage. The generated poses were energy minimized using the MMFF94x force field. Finally, the optimized poses were ranked using the GBVI/WSA DG free-energy estimates as shown in Table 1. (Naïm et al., 2007). Docking poses were visually inspected and interactions with binding pocket residues were analyzed.

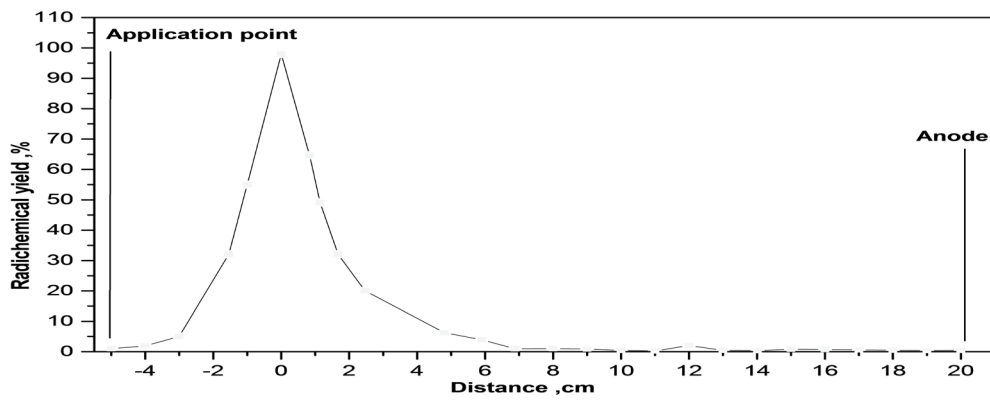


Fig.3. Electrophoresis of ¹³¹I- aniracetam complex at optimum conditions

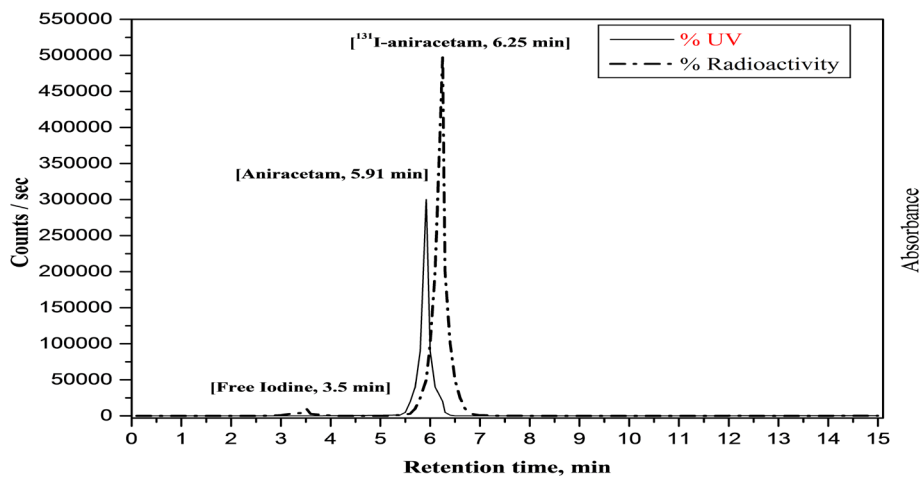


Fig. 4. HPLC radiochromatogram of ¹³¹I- aniracetam complex

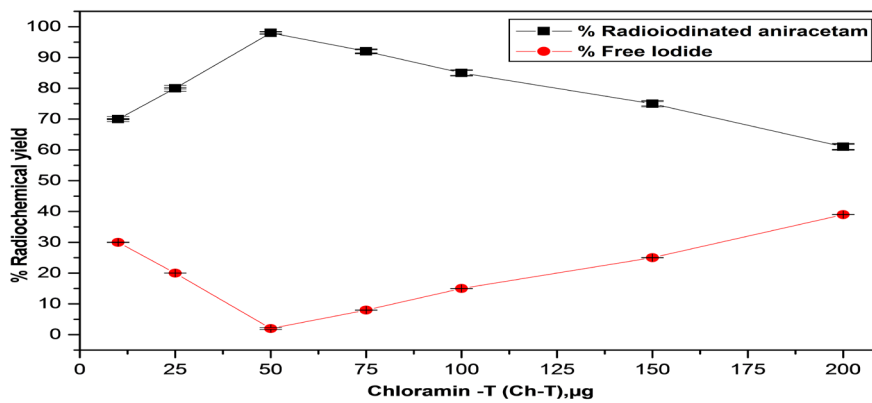


Fig. 5. The effect of oxidizing agent on the radiochemical yield reaction conditions: 10µl (~3.7MBq) Na¹³¹I, 100 µg of aniracetam, (x µg) of Ch-T, at pH 6, the reaction mixtures were kept at room temperature for 30 min.

Results

The pH of the reaction mixture, amount of the oxidizing agent (chloramine-T (Ch-T)), amount of the ligand, and reaction time of the mixture were optimized at ambient temperature. Figure 5 shows that the conversion to radioiodinated aniracetam increased up to a ceiling of 50 μg of Ch-T giving an optimum radiochemical conversion of 98.0%, other reaction parameters were kept constant. Excess Ch-T may lead to the formation of undesirable oxidative by-products such as chlorination and polymerization. Hence 50 μg of Ch-T (~1.5eq.) gave the optimum conversion to iodo aniracetam (Sanad *et al.*, 2016). The effect of changing substrate to iodide ratio is shown in figure 6 which reveals that the optimum radiochemical conversion to radioiodinated aniracetam (98.0%) at 100 μg of aniracetam and [^{125}I] Na (7.5MBq). In addition, pH is an important factor in radio-iodination (see Figure 7) which needs to be controlled, pH 6 proved to be optimal which may be reflected in part the stability of radioiodinated aniracetam (Sanad *et al.*, 2016). The effect of reaction time was also studied giving a maximum conversion at 30 min. (Figure 8). The in-vitro stability of iodonzitidine (Fig. 9) was studied in two different media. It was found to be stable in saline for up to 48 hours. In contrast, in serum after 24 hours, the purity dropped to 94.0 % then decreased to 94 % at 48 h. The logarithm of the partition coefficient ($\log p$) value of [^{125}I] aniracetam was 2.11 ± 0.01 that demonstrated its ability to cross the blood brain barrier. Finally, Drug inhibition study indicated that the different amounts of unlabelled aniracetam used, 15 min before the injection of [^{125}I] aniracetam decreased the brain uptake ratio from 9.50 to 1.55 % ID/g organ at 15 min p.i. (Fig. 10). This result indicates that [^{125}I] aniracetam binds selectively to AMPA receptors located in the brain.

Gamma scintigraphy imaging results, as shown in Fig. 11, the biodistribution of [^{131}I] aniracetam accumulated into the brain of mice reached its maximum in 15 minutes p.i..

The biodistribution of radioiodinated aniracetam as shown in Table 4, demonstrated that important body organs and fluids were represented as percent-injected dose per gram \pm S.E.M. (%ID/gram). The radioactivity accumulated in the thyroid should be referred to the in vivo instability of radioiodinated aniracetam. Therefore low activity uptakes in thyroid indicated that this radiotracer was *Egypt. J. Rad. Sci. Applic.*, Vol. 30, No.1(2017)

considered stable in vivo. The liver up takes increased from 19.15 at 5 min post injection (p.i.) to 33.25 at 30 min post injection and declined at 4 hours to give 7.12(%ID/gram), therefore, the labeled compound was excreted through hepatobiliary pass way and it was considered lipophilic radiotracer (Zhang *et al.*, 2007). Kidneys uptake increased from 3.4 % at 5 min post injection to 5.60 % at 30 min post injection that declined to 1.01% at 4 h post injection. The brain uptake of radioiodinated aniracetam was 7.9, 9.5, 6.0, 4, 2.3 and 1.6 at 5, 15, 30 min, 1h, 2h and 4h (%ID/gram) respectively. The high uptake of the radiotracer at 15 min can be noticed in gamma scintigraphy images (Fig. 11). Additionally, the brain/blood ratios were 0.80 at 5 min to 2.01 at 4 h which was a good ratio to image brain compared to other radiotracers (Fig. 12.).

Molecular modeling studies were advocated by self-docking in the AMPA crystal structure (PDB code 4UQK), by eliminating the bound ligand, QUS, from the radiotracer after that docking it back into the binding site and the main interactions showed that it has ten hydrogen bonds with the key amino acids ARG485, THR480, SER654, THR655, GLU705 and PRO478 also it has a π -interaction with TYR450 as shown in Table 2. Furthermore, the top ranked pose exhibited heavy-atom root-mean-square deviation (RMSD) value of 0.346 Å from the experimental crystal structure.

Discussion

Reaction optimization of [^{125}I] aniracetam gave a high radiochemical yield, high stability in two different media, and also [^{125}I] aniracetam binds selectively to AMPA receptors located in the brain that was indicated by Molecular Operating Environment (MOE) docking that can reliably predict docking poses for the studied compounds to AMPA. The binding affinity of the ligand and the tested compounds were evaluated with S-score. The minimum the docking score is the higher the binding affinity is to the enzyme complex. Interactive docking using MOE protocol was carried out between the predicted structures and the prepared AMPA receptor. Each proposed structure gave 10 possible docked poses. The main one of each molecule can be elected by the uniformity of its binding format in the binding site to that of the ligand QUS. The results of the docking study including S-score, interacted amino acids and the length of H-bonds formed of all the

compounds and the reference ligand are listed in Table 3. Generally, MOE docking gave the top-ranked poses indicated that both aniracetam and [^{125}I]aniracetam can interact with 4UQK in a very similar manner like QUS as shown in Table 2, 3. The docking and binding affinity of aniracetam to the receptor pocket has S-score of -14.0338 kcal/mol and exhibited five hydrogen bonds: one with ARG485 of distance (2.8 Å), two with SER654 of distance (2.6, 2.69 Å), one with THR655 of distance (2.86 Å) and last with THR686 of distance (2.95 Å). While, the docking and binding affinity of [^{125}I]aniracetam to the receptor pocket has S-score of -15.6342 kcal/mol indicating that the binding of [^{125}I]aniracetam is better than aniracetam. Moreover, [^{125}I]aniracetam exhibited five hydrogen bonds: Two with THR686 of distance (2.8, 2.64 Å), two with SER654 of distance (2.46, 2.82 Å), one with TYR702 of distance (2.64 Å) and also it has a π -interaction with TYR450. Conclusively, introduction of heavy iodine atoms improved binding of aniracetam to its target receptor (4UQK). From biodistribution study, radioiodinated aniracetam was considered more than other complexes used such as $^{99\text{m}}\text{Tc}$ -piracetam that gave 4.9 ± 0.1 % ID/organ (Amin et al., 2013). In addition, $^{99\text{m}}\text{Tc}$ -ropinirole, ^{125}I -fluoxetine, ^{125}I -sibutramine, $^{99\text{m}}\text{Tc}(\text{CO})_3$ -5HTIDA and $^{99\text{m}}\text{Tc}(\text{CO})_3$ -DEDT that showed 4.7, 1.29, 3.19, 0.25 and 1.41%ID/g at 30 min post injection in mice, respectively. Also, agents such as $^{99\text{m}}\text{Tc}$ -HMPAO and $^{99\text{m}}\text{Tc}(\text{CO})_3$ -

OH-PP-CS₂ that showed 2.25 and 0.32 %ID/g at 30 min post injection in rats, respectively. Finally radioiodinated aniracetam higher than that $^{99\text{m}}\text{Tc}$ -tricarbonyl oxiracetam complex (Sanad, et al 2017) and $^{99\text{m}}\text{Tc}$ -ECD complex that showed 7.5 ± 0.11 % ID/g at 5 min post injection in mice and 4.7 %ID/g at 24 hr post injection in monkey respectively (Motaleb et al 2016; Motaleb et al., 2011; Satpati et al., 2006; Zhang et al., 2007; Neirincx et al., 2012; Erfani et al., 2012; Walovitch et al., 1989). From above data, it was concluded that radioiodinated aniracetam has brain uptake at 15 min p.i. more than all above complexes. Therefore, radioiodinated aniracetam could be used to brain imaging than others according to its receptors (AMPA).

Conclusion

An optimized protocol for the synthesis of radioiodinated aniracetam in high yield has been elaborated. Biodistribution studies indicated that radioiodinated aniracetam has a high brain uptake of 9.5 % ID/g at 15 min. that was confirmed by gamma camera and binding with AMPA receptors. The radiotracer radioiodinated aniracetam considers more better than recently discovered agents such as [$^{99\text{m}}\text{Tc}$] piracetam, [$^{99\text{m}}\text{Tc}$]tricarbonyl oxiracetam complex, [$^{99\text{m}}\text{Tc}$](CO)₃-5HTIDA, [$^{99\text{m}}\text{Tc}$](CO)₃DEDT and [$^{99\text{m}}\text{Tc}$](CO)₃-OH-PP-CS₂, [$^{99\text{m}}\text{Tc}$]ropinirole, [$^{99\text{m}}\text{Tc}$]ECD and [$^{99\text{m}}\text{Tc}$]HMPAO complexes have.

TABLE 1. Aniracetam and ^{125}I -aniracetam proposed structure after energy minimization

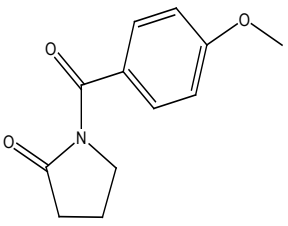
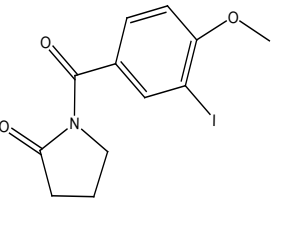
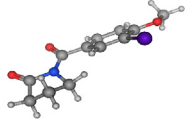
Compound	2D format	3D after energy minimization
Aniracetam		
^{131}I -aniracetam Proposed structure		

TABLE 4. Biodistribution of [¹²⁵I]aniracetam in normal mice at different times

Organs & body fluids	% I.D./gram at different times post injection					
	5 min	15 min	30 min	60 min	120 min	240 min
Blood	10.0 0.11 ±	7.9 0.17 ±	4.1 0.15 ±	2.3 0.19 ±	1.2 0.17 ±	0.77 0.00 ±
Bone	2.1 0.15 ±	1.7 0.13 ±	1.1 0.11 ±	1.0 0.16 ±	0.9 0.00 ±	0.91 0.11 ±
Muscle	4.1 0.11 ±	3.9 0.15 ±	3.2 0.22 ±	2.8 0.22 ±	0.95 0.00 ±	0.80 0.00 ±
Brain	7.9 0.12 ±	9.5 0.77 ±	6.0 0.86 ±	4.0 0.28 ±	2.3 0.22 ±	1.6 0.13 ±
Lungs	1.0 0.13 ±	1.2 0.16 ±	1.3 0.11 ±	1.0 0.13 ±	0.9 0.00 ±	0.91 0.00 ±
Heart	1.2 0.13 ±	1.0 0.14 ±	0.9 0.00 ±	0.8 0.00 ±	0.77 0.00 ±	0.58 0.00 ±
Liver	19.15 1.12 ±	25.35 1.26 ±	33.25 1.22 ±	18.21 1.01 ±	12.10 1.17 ±	7.12 0.99 ±
Kidneys	3.4 0.66 ±	4.5 0.29 ±	5.6 0.11 ±	2.14 0.23 ±	1.95 0.21 ±	1.01 0.28 ±
Spleen	0.88 0.00 ±	1.0 0.00 ±	1.5 0.13 ±	0.9 0.00 ±	0.7 0.00 ±	0.66 0.00 ±
Intestine	5.5 0.55 ±	8.1 0.32 ±	10.1 0.34 ±	18.21 0.96 ±	15.01 1.11 ±	8.2 0.56 ±
Stomach	1.1 0.10 ±	1.3 0.11 ±	1.2 0.24 ±	0.9 0.00 ±	0.9 0.00 ±	0.9 0.00 ±
Brain/Blood	0.80	1.20	1.46	1.74	1.92	2.01

Mean ± SEM (mean of five experiments)

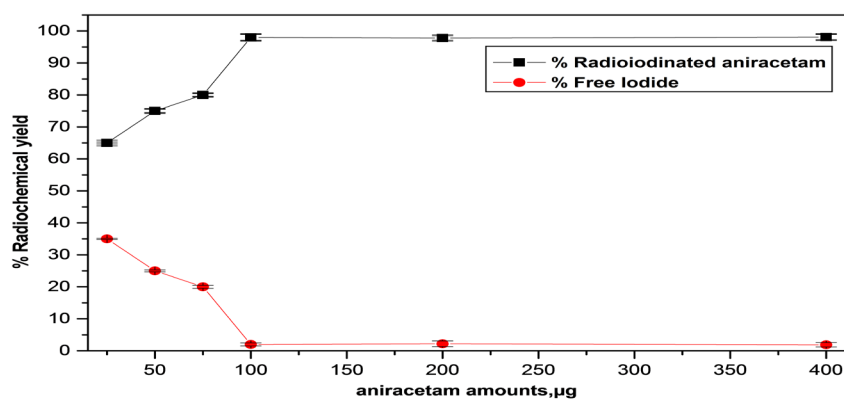


Fig. 6. Variation of the radiochemical yield of ¹³¹I-aniracetam as a function of different aniracetam amounts; reaction conditions: 10 μl (~3.7 MBq) Na¹³¹I, x μg aniracetam, 50 μg of Ch-T, at pH 6, the reaction mixtures were kept at room temperature for 30 min.

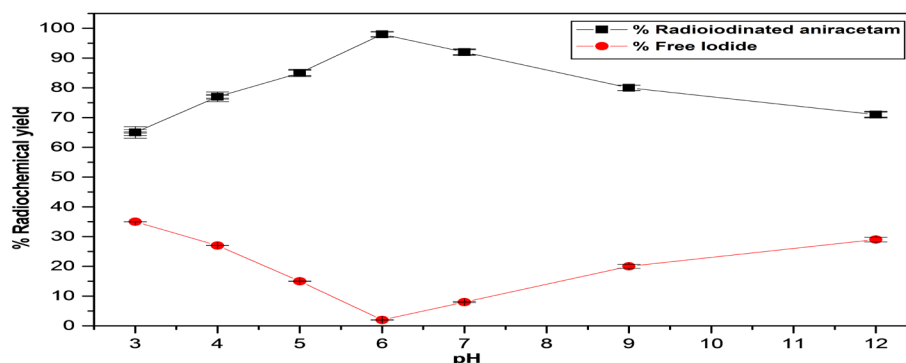


Fig. 7. Variation of the radiochemical yield of ¹³¹I-aniracetam as a function of pH; reaction conditions: 10 μl (~3.7 MBq) Na¹³¹I, 100 μg of aniracetam, 50 μg of Ch-T, at different pH, the reaction mixtures were kept at room temperature for 30 min.

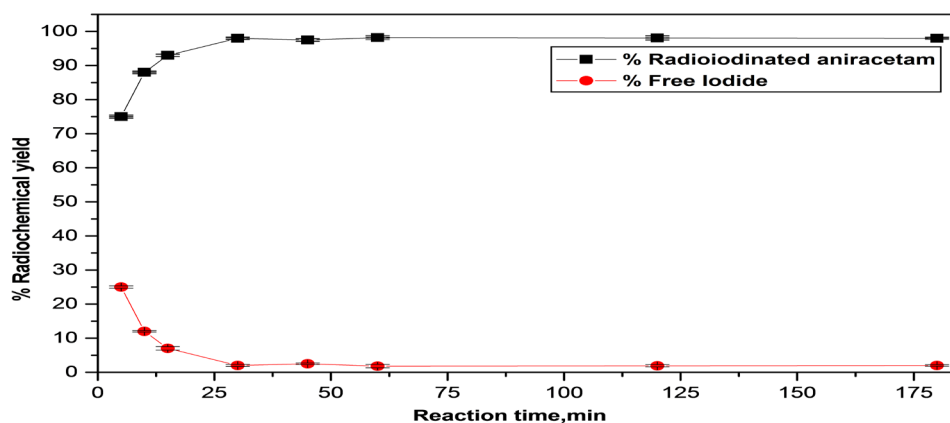


Fig. 8. Variation of the radiochemical yield of ^{131}I -aniracetam as a function of reaction time; reaction conditions: $10\ \mu\text{l}$ ($\sim 3.7\ \text{MBq}$) Na^{131}I , $100\ \mu\text{g}$ of aniracetam, $50\ \mu\text{g}$ of Ch-T, at pH 6, the reaction mixtures were kept at room temperature for 30 min.

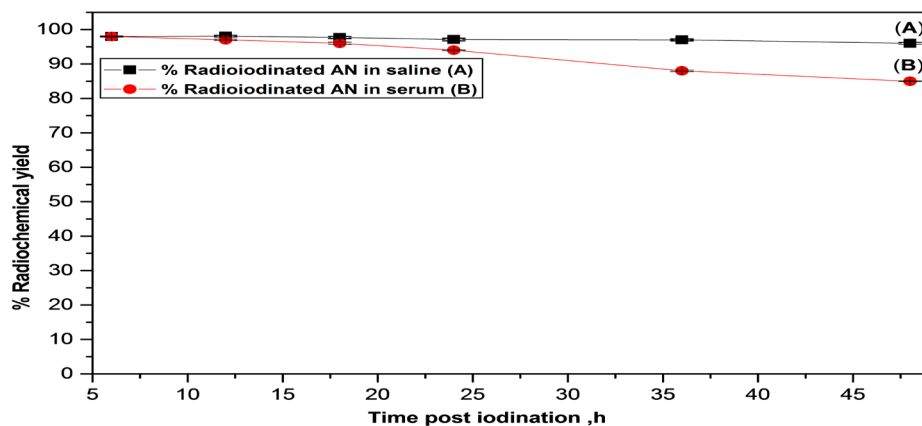


Fig. 9. In vitro stability of ^{131}I -aniracetam in saline (A) and serum (B).

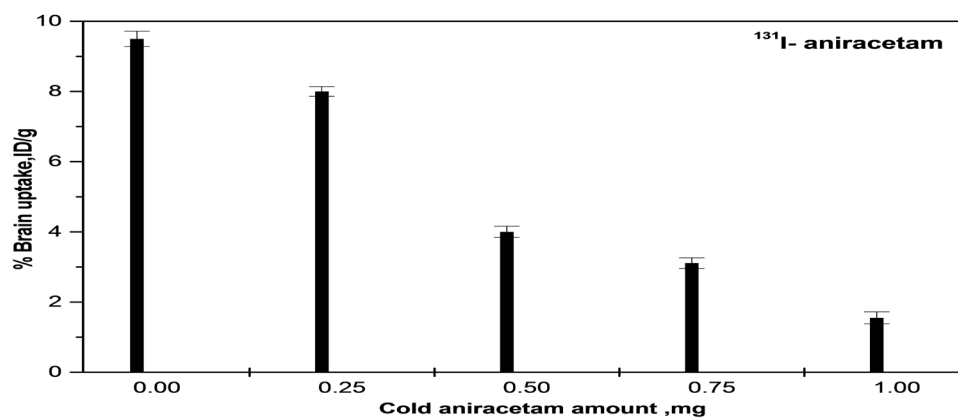


Fig. 10. Radioiodinated aniracetam inhibition brain uptakes in normal male Swiss Albino mice at 15 min p.i. (% ID/gram \pm SEM, $n = 5$)

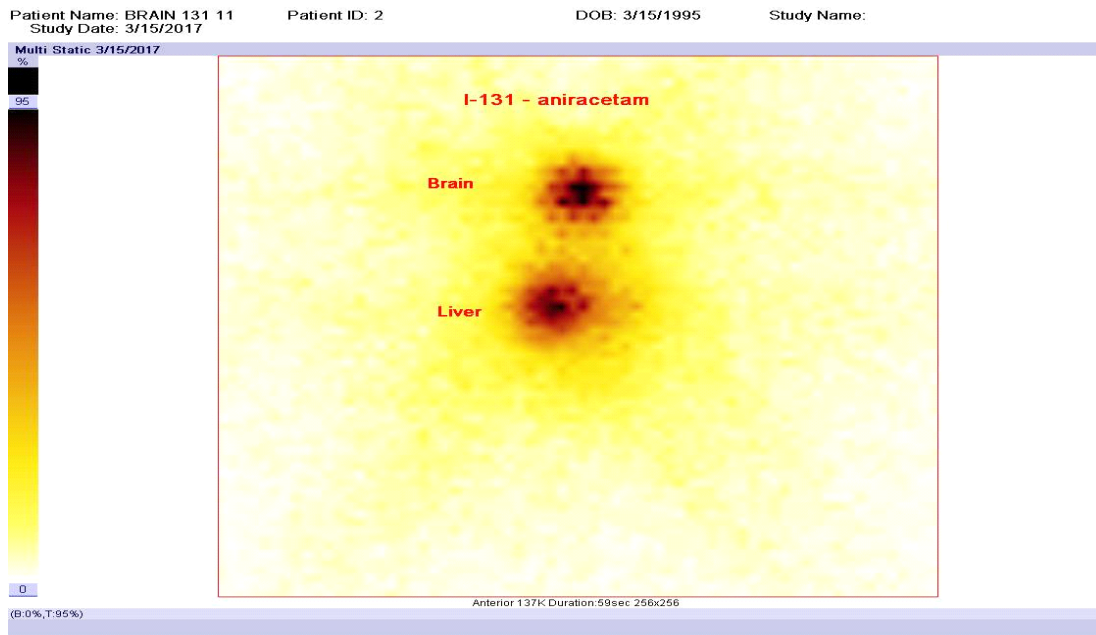


Fig. 11. Scintigraphy image showing the brain uptake of ^{131}I - aniracetam.

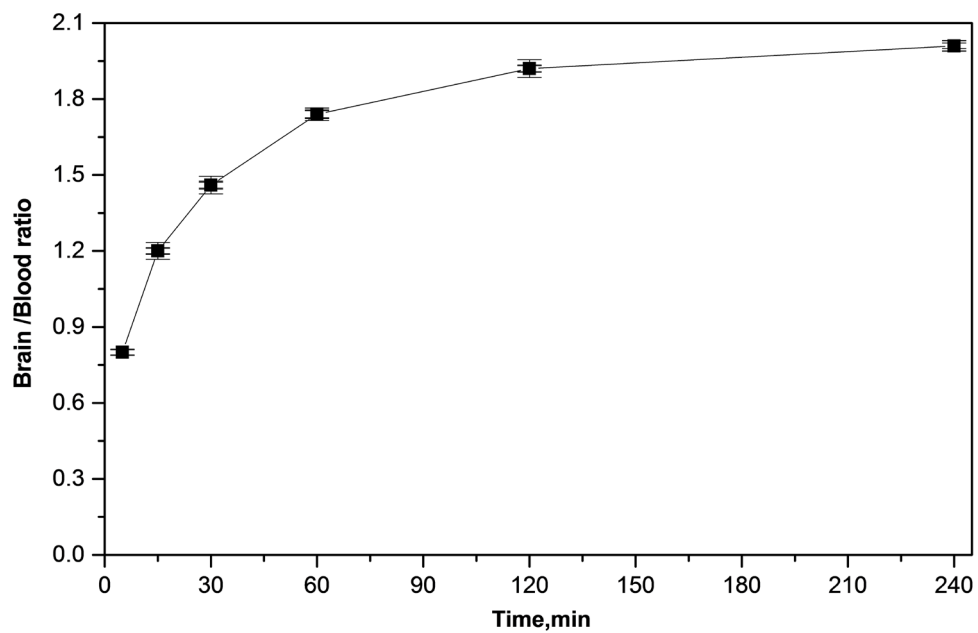


Fig. 12. Brain/blood ratio of radioiodinated aniracetam in normal male Swiss Abino mice as a function of time

References

- Amin, A. M., Sanad, M. H., Abd-Elhalim, S.M. (2013) Radiochemical and Biological Characterization of ^{99m}Tc -piracetam for Brain Imaging. *J Nucl Med* **55**(6), 624–628
- Bateman, T.M. (2012) Advantages and disadvantages of PET and SPECT in a busy clinical practice. *J Nucl Cardiol. Suppl* 1:S3-11. doi: 10.1007/s12350-011-9490-9.
- Bowie, D. (2012) Redefining the classification of AMPA-selective ionotropic glutamate receptors. *J Physiol* **590** (1): 49-61
- Bruno, J. R. N. (1982) Chemistry and pharmacological of nootropics. *Drug Dev Res.* **2**(5):463-474.
- Eggebrecht, A.T., White, B.R., Ferradal, S.L., Chen, C., Zhan, Y., Snyder, A.Z., Dehghani, H. and Culver, J.P. (2012) A quantitative spatial comparison of high-density diffuse optical tomography and fMRI cortical mapping. *Neuroimaging* **61** (4):1120–8.
- Eleore, L., Vassias, I., Vidal, P.P., de Waele, C. (2005) Modulation of the glutamatergic receptors (AMPA and NMDA) and of glutamate vesicular transporter in the rat facial nucleus after axotomy. *Neuroscience* **136**(1): 147-60.
- Erfani, M., Hassanzadeh, L., Ebrahimi, S.E.S., Shafiei, M. (2012) Synthesis and biological evaluation of ^{99m}Tc (CO)₃-OH-PP-CS₂ for brain receptor imaging *Iran. J Nucl Med.* **20** (1):25–31
- Farid, K., Petras, S., Ducasse, V., Chokron, S., Helft, G., Blacher, J., et al. (2012) Brain perfusion SPECT imaging and acetazolamide challenge in vascular cognitive impairment. *Nucl Med Commun.* **33** (6):571-80.
- Heilbrun, M.P., Sunderl, P.M., McDonald, P.R., Wells, T.H., Cosman, E., Ganz, E. (1987) Brown-Roberts-Wells stereotactic frame modifications to accomplish magnetic resonance imaging guidance in three planes". *Applied Neurophysiology* **50** (1–6): 143–152.
- Hupf, H.B., Eldridge, J.S., Beaver. (1968) Reproduction of iodine-123 for medical applications". *Int J Appl Radiat Isot.* **19** (4): 345–51.
- Kamlesh, M. P., Upendra, R. P., Pradhuman, A. P., Ashaben, D. P. (2016) Development and validation of a reversed-phase HPLC method for the simultaneous determination of aniracetam and impurities in the bulk drug. *IJAPBC* **5** (2): 220-232
- Labute, P. (2008) Protonate 3D: assignment of ionization states and hydrogen coordinates to macromolecular structures, *Proteins* **75**: 187-205.
- Levivier, M., Massager, N., Wikler, D., Lorenzoni, J., Ruiz, S., Devriendt, D., David, P., Desmedt, F., Simon, S., Van Houtte, P., Brotchi, J., Goldman, S. (2004) Use of stereotactic PET images in dosimetry planning of radiosurgery for brain tumors: clinical experience and proposed classification. *Journal of Nuclear Medicine* **45** (7): 1146–1154.
- Maina, G., Fiori, L., Torta, R., Fagiani, M.B., et al. (1989) Oxiracetam in the Treatment of Primary Degenerative and Multi-Infarct Dementia: A Double-Blind, Placebo-Controlled Study. *Neuropsychobiology* **21**: 141–145
- Molecular Operating Environment (MOE), (2013) 2008.10., Chemical Computing Group Inc., 1010 Sherbooke St. West, Suite #910, Montreal, QC, Canada., H3A, 2R7.
- Motaleb, M.A., Ibrahim, I.T., Ayoub, V.R., Geneidi, A.S. (2016) Preparation and biological evaluation of ^{99m}Tc -ropinirole as a novel radiopharmaceutical for brain imaging. *J Label Compd Radiopharm.* **59**(4): 147-52.
- Motaleb, M.A., El-Kolaly, M.T., Rashed, H.M., Abd El-Bary, A. (2011) Novel radioiodinated sibutramine and fluoxetine as models for brain imaging. *J Radioanal Nucl Chem.* **289**(3):915-921.
- Naïm, M., Bhat, S., Rankin, K. N., Dennis, S., Chowdhury, S. F., Siddiqi, I., Drabik, P., Sulea, T., Bayly, C. I., Jakalian, A. and Purisima, E. O. (2007) Solvated interaction energy (SIE) for scoring protein-ligand binding affinities. 1. Exploring the parameter space, *J. Chem. Inf. Model.* **47**:122-133.
- Neirinckx, R.D., Canning, L.R., Piper, I.M., Nowotnik, D.P., Pickett, R.D., Holmes, R.A., Volkert, W.A., Forster, A.M.,
- Weisner, P.S., Marriott, J.A., Chaplin, S.B. (1987) Technetium-99m d, l-HM-PAO: a new radiopharmaceutical for SPECT imaging of regional cerebral blood perfusion. *J. Nucl. Med.* **28**:191–202
- Ozawa, S., Kamiya, H., Tsuzuki, K. (1998) Glutamate receptors in the mammalian central nervous system. *Prog Neurobiology* **54**(5):581-618.
- Sanad, M.H, Sakr, T.M., Walaa, H.A.F., Marzook, E.A. (2016) In silico study and biological evaluation of ^{99m}Tc -tricarbonyl oxiracetam as a selective imaging probe for AMPA receptors. *J. Radioanal. Nucl. Chem.* DOI 10.1007/s10967-016-5120-y

- Sanad, M.H., Sallam, Kh. M., Marzook, F.A. and Abd-Elhaliem, S.M. (2016) Radioiodination and biological evaluation of candesartan as a tracer for cardiovascular disorder detection. *J. Label Compd. Radiopharm.* **59**: 484-491.
- Sanad, M. H., Salama, D. H. and Marzook ,F.A. (2017) Radioiodinated famotidine as a new highly selective radiotracer for peptic ulcer disorder detection, diagnostic nuclear imaging and biodistribution. *Radiochim. Acta* **105**(5):389-398.
- Satpati, D., Bapat, K., Mukherjee, A., Banerjee, S., Kothari, K., Venkatesh, M. (2006) Preparation and bioevaluation of ^{99m}Tc-carbonyl complex of 5-hydroxy tryptamine derivative. *Appl. Rad. Isot.* **64** (8):888-892
- Simon, S. L., Bouville, A. L., Charles, E. (2006) Fallout from Nuclear Weapons Tests and Cancer Risks". *American Scientist* **94**: 48-57.
- Silberstein, S. D. (2000) Practice parameter: Evidence-based guidelines for migraine headache (an evidence-based review): Report of the Quality Standards Subcommittee of the American Academy of Neurology. *Neurology*, **55** (6): 754-762.
- Stensbol, T.B., Madsen, U., Krogsgaard-Larsen, P. (2002) The AMPA receptor site: Focus on agonists and competitive antagonists *Curr. Pharm. Des.* **8**(10):857-872.
- Thomas, D.G., Anderson, R.E., du Boulay, G.H. (1984) CT-guided stereotactic neurosurgery: experience in 24 cases with a new stereotactic system. *J. Neurol Neurosurg Psychiatry* **47**(1): 9-16.
- Venkat, R., Narra, R., Howell, W., Raw, S. H., Kandula, S. R. S., Dandamudi, V. R. (1992) Radiotoxicity of Some Iodine-123, Iodine-125 and Iodine-131-Labeled Compounds in Mouse Testes: Implications for Radiopharmaceutical *Design. J Nucl Med.* **33**: 2196-2201.
- Walovitch, R.C., Hill, T.C., Garrity, S.T., Cheesman, E.H., Burgess, B.A., O'leary, D.H., Watson, A.D., Ganey, M.V., Morgan, R.A., Williams, S.J. (1989) Characterization of technetium-99m-L, L-ECD for brainperfusion imaging. Part 1: pharmacology of technetium-99mECD in nonhuman primates. *J. Nucl. Med.* **30** : 1892 -1901.
- Zhang, J., Wang, X., Jin, C. (2007) Synthesis and biodistribution of the ^{99m}Tc (CO)₃-DEDT complex as a potential new radiopharmaceutical for brain imaging. *J. Radioanal. Nucl. Chem.* **272**(1):91-94.

Received 18/ 8/ 2017;
accepted 13/11/2017)

الترقيم باليود المشع والنمذجة الجزيئية والتقييم البيولوجي للأنيروستام كمتعاقب للتصوير المشع للمخ

*محمود حمدى محمود سند ،ايمن عبد الفتاح بسطاوى فرج و دينا حسيني سلامة
*قسم المركبات المرقمة- مركز المعامل الحارة - هيئة الطاقة الذرية- قسم
الكيمياء الصيدلانية- كلية الصيدلة - جامعة الأهرام الكندية- قسم البحوث الصحية الإشعاعية - المركز القومي
لبحوث و تكنولوجيا الإشعاع- هيئة الطاقة الذرية - مصر.

تركز الدراسة الحالية على تحضير الأنيروستام المرقم باليود المشع لأمكانية تصوير المخ. تم ترقيم الأنيروستام باليوم-125 وكذلك اليود-131 باستخدام الكلورامين-ت كعامل مؤكسد. ومن العوامل الفعالة الرئيسية المستخدمة مثل كمية العامل المؤكسد ، كمية المادة المستخدمة، الأس الهيدروجيني، درجة حرارة التفاعل و زمن التفاعل حيث تم دراسة كل ذلك تباعا لكي يعطى أعلى عائد ترقيمي للأنيروستام المشع. حيث سجلت النتائج أعلى عائد ترقيمي للأنيروستام المشع وصلت لنسبة 98٪. تم فصل المركب المرقم وكذلك تم تنقيته باستخدام كروماتوجرافيا السوائل ذات الضغط العالي ، تقنية الكروماتوجرافيا الورقية والفصل بالتحليل الكهربى ذات الجهد. كما تم دراسة كلا من النمذجة والالتحام مع المستقبل - AMPA ، كذلك التصوير بالجمال كاميرا و تثبيط المادة المشعة باستخدام المادة نفسها فى الحالة الغير مشعة. وتم دراسة التوزيع البيولوجى للمتركب باستخدام فئران التجارب. والتي أوضحت أن المتركب يتمركز بالمخ بنسبة 9,5 ٪ عند 15 دقيقة بعد الحقن . بناء على تلك النتائج من الممكن اعتبار هذا المتركب من المواد التى يمكن أن تستخدم بكفاءة فى أقتفاء التصوير الأشعاعى للمخ.